

CAPTURABILITY OF INVERTED PENDULUM GAIT MODEL UNDER SLIP CONDITIONS

Marko Mihalec and Jingang Yi

Department of Mechanical and Aerospace Engineering Rutgers the State University of New Jersey Piscataway, New Jersey 08854 Email: {marko.mihalec, jgyi}@rutgers.edu

ABSTRACT

This paper presents a simple inverted pendulum gait model to study walking under slip conditions. The model allows for both the horizontal and vertical movements of the center of mass during normal walking and walking gaits with foot slip. Stability of the system is analyzed using the concept of capturability. Considering foot placement as a control input, we obtain the stable regions which lead to stable gait. The size of those stable regions is used to evaluate the effect of the coefficient of friction and the slip reaction time on capturability. We also analyze the feasibility of recovery from slip gait in relation to the coefficient of friction and the reaction time. The results confirm the effectiveness of the model and the capturability developement.

INTRODUCTION

Fall-related injuries are the largest contributor to the economic burden of injuries among the elderly in the US [1]. In the general population, the fall-related injuries are second only to motor vehicle injuries when it comes to lifetime costs [2]. Numerous studies have been conducted to examine fall [3,4]. However, majority of such studies focus on clinical experiments to describe the variables for the onset of slip and to detect such occurrences [5,6]. In order to better understand the fundamentals of bipedal walking and slip, various simplified analytic models have been presented [7–9]. This kind of abstract models have been developed from simple single inverted pendulums (LIP) [10,11], to the more complex models that are obtained by stacking together multiple pendulums [12, 13]. In order to reduce the com-

plexity, the majority of models use simplified, linear dynamics (e.g., [14]). Such a simplification neglects the vertical motion of mass, which is a critical part of slip gait. Hence, a model which allows for the vertical movement of mass, similar to [15] is needed to study walking gait with foot slip. Many walking models require a non-slip condition between the ground and the foot. Planning approaches have been proposed under non-slip conditions [16] to ensure compliance with slip restrictions [17]. On the other hand, some models allow slip conditions by incorporating friction into their dynamics, such as [18] the two mass LIP model in [19].

Stability is one of the main research topics for bipedal walkers. Dynamic stability [20] examines the relation of the center of mass (COM) to the size of the support base of the walker. To better describe the concept of stability during walking gait, the concept of divergent component of motion (DCM) or capture point (CP) was introduced in [21] and later expanded [22, 23]. Along with the capture point, the capture region is defined as the region where a foot can be placed in order to bring a biped to stop in a single step. Capture regions are extended by omitting a single step requirement and thereby obtaining the concept of capturability [24]

This work presents a simple inverted pendulum model to incorporate vertical movement as well as a slip contact condition. First, the non-linear dynamics are presented for both non-slip and slip conditions. A model is presented to describe multiple steps and the concept of capturability. We then present the capturability analysis as a function of different parameters such as the friction coefficient and walker's reaction time. The main con-

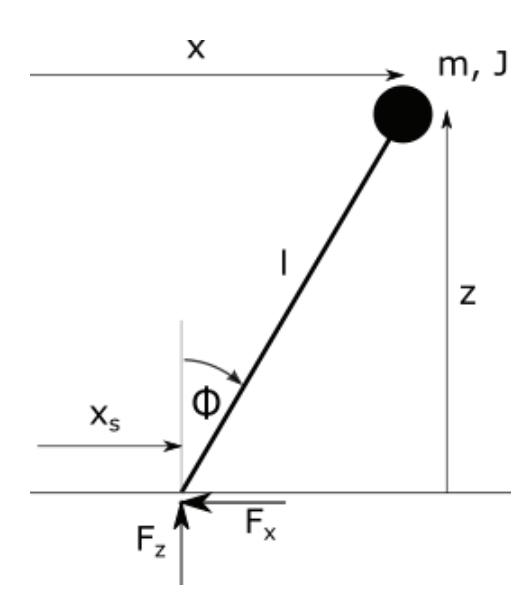


FIGURE 1. The inverted pendulum model for bipedal walkers

tribution of this work is to apply the concept of capturability to walking gaits with foot slip. Capture regions are calculated and the effects of varying the friction coefficient and the time between steps are presented.

PENDULUM MODEL DYNAMICS

When considering normal walking without slip, it is assumed that the contact point between the pendulum and the ground is stationary. In order to simplify the model, it is usually assumed that the COM stays at constant height. When dealing with slip, both of those assumptions have to be relaxed in order to sufficiently describe the motion.

The model used in this work considers a constant length l inverted pendulum, with mass m and a moment of inertia J around the COM. Figure 1 shows the model schematic of the biped walker. The Cartesian location of the COM is denoted in the ground fixed xz frame and ϕ denotes the angle of the pendulum from the vertical position. Mass m represents the concentrated mass of the entire body, while moment J represents the mass moment of inertia of the pendulum and the reaction forces at the point of contact are denoted as F_x in horizontal and F_z in vertical direction. No ankle actuation is considered in the model.

Dynamics without slip

In the case when no slip occurs and the contact point is stationary, the dynamics equation in the horizontal, vertical and ro-

tational directions are given respectively as follows,

$$\ddot{x} = -\frac{F_x}{m},\tag{1}$$

$$\ddot{z} = \frac{F_z}{m} - g,\tag{2}$$

$$\ddot{\phi} = \frac{F_z l}{I} \sin \phi + \frac{F_x l}{I} \cos \phi. \tag{3}$$

Combining Eqs. (1) - (3). we eliminate the reaction force variables and obtain a single equation

$$\frac{J}{ml}\ddot{\phi} = \ddot{z}\sin\phi - \ddot{x}\cos\phi + g\sin\phi \tag{4}$$

Since the contact point is always on the ground and is stationary, variables x and z can be expressed as

$$x = l\sin\phi, \qquad z = l\cos\phi \tag{5}$$

Taking time derivatives of Eq. (5) and substituting them into Eq. (4), a final form of dynamic equation is obtained:

$$\ddot{\phi} = \frac{mlg\sin\phi}{J + ml^2} \tag{6}$$

Dynamics under slip When the contact point experiences slip, the governing Eqs. (1), (2) and (3) still hold. Since the standing leg does not leave the ground during slip, relationship in z is still Eq. (5) is still held.

The relationship in Eq. (5) describes the relation between x and the angle ϕ in the non-slip case and is not valid under foot slip. Rather, x is treated as a state variable and describes the horizontal distance between the center of mass and the foot initial contact point.

During the slip phase, a simple friction relation between the reaction forces is assumed $F_x = \mu F_z \operatorname{sign}(\dot{x}_s)$, where μ is a friction coefficient and $\operatorname{sign}(\dot{x}_s)$ equals to 1 and -1 when $\dot{x}_s > 0$ and $\dot{x}_s < 0$, respectively. The dynamic equations under slip conditions are then written as

$$\ddot{\phi} = -\frac{lm\ddot{x}}{J\mu} \left(\operatorname{sgn}(\dot{x}) \sin \phi + \mu \cos \phi \right), \tag{7}$$

$$\ddot{x} = \operatorname{sgn}(\dot{x}) \, \mu \, \left(l \ddot{\phi} \sin \phi + l \dot{\phi}^2 \cos \phi - g \right), \tag{8}$$

or alternatively in explicit form:

$$\ddot{\phi} = \frac{\operatorname{sgn}(\dot{x}) m l (g - l \dot{\phi}^2 \cos \phi) (\operatorname{sgn}(\dot{x}) \sin \phi + \mu \cos \phi)}{J + \operatorname{sgn}(\dot{x}) l^2 m \sin \phi (\operatorname{sgn}(\dot{x}) \sin \phi + \mu \cos \phi)}, \quad (9)$$

$$\ddot{x} = \frac{\operatorname{sgn}(\dot{x})J\mu(l\dot{\phi}^2\cos\phi - g)}{J + \operatorname{sgn}(\dot{x})l^2m\sin\phi(\operatorname{sgn}(\dot{x})\sin\phi + \mu\cos\phi)}.$$
 (10)

If we choose x_s as the state variable, namely

$$x = x_s + l\sin\phi. \tag{11}$$

Eq. (10) is then rewritten as

$$\ddot{x}_s = \ddot{x} + l\,\dot{\phi}^2\sin\phi - l\,\ddot{\phi}\cos\phi\tag{12}$$

or explicitly:

$$\ddot{x}_{s} = \frac{l \operatorname{sgn}(\dot{x})(\operatorname{sgn}(\dot{x}) \sin \phi + \mu \cos \phi)(J\dot{\phi}^{2} + ml^{2}\dot{\phi}^{2} - mgl \cos \phi)}{J + \operatorname{sgn}(\dot{x})l^{2}m \sin \phi (\operatorname{sgn}(\dot{x}) \sin \phi + \mu \cos \phi)} - \frac{\operatorname{sgn}(\dot{x})gJ\mu}{J + \operatorname{sgn}(\dot{x})l^{2}m \sin \phi (\operatorname{sgn}(\dot{x}) \sin \phi + \mu \cos \phi)},$$
(13)

Slip often happens at the moment the heel strikes the ground but may also occur at any other moments of gait phase. Given a set of state variables $(\phi, \dot{\phi}, x_s, \dot{x}_s)$, if $\dot{x}_s = 0$, Eq. (6) is used to compute $\ddot{\phi}$. Then, by combining Eqs. (1), (2) with (5) and (??), we calculate reaction forces as:

$$F_x = ml(\dot{\phi}^2 \cos \phi + \ddot{\phi} \sin \phi), \tag{14}$$

$$F_z = mg - ml(\dot{\phi}^2 \sin \phi + \ddot{\phi} \cos \phi). \tag{15}$$

To maintain the contact with the ground, $F_z > 0$ is required for any valid gait. Next, it is verified whether the coefficient of friction is sufficient. If $|F_x| < \mu F_z$, the friction at the contact point is sufficient so that slip does not occur and $\dot{x}_s = \ddot{x}_s = 0$. If $|F_x| > \mu F_z$ or $\dot{x}_s \neq 0$, the system is under slip and Eqs. (9) and (13) are used to compute the dynamics.

Multiple steps

To describe continuous and discrete changes between two steps, subscript f is used to denote the final value of a variable from previous step, while subscript i denotes the initial value in the next step. During a single step, the dynamics is predicted as an initial value problem with initial values x_{si} , \dot{x}_{si} , ϕ_i and $\dot{\phi}_i$ and governed by Eqs. (9) and (10). A single step is assumed to have

a fixed duration of t_1 , so that after time t_1 , the values for the state variables are x_{sf} , \dot{x}_{sf} , ϕ_f and $\dot{\phi}_f$.

In order to initiate the next step, the position of the stance foot is instantaneously reassigned and consequently, a discrete jump from ϕ_f to ϕ_i is enforced. Since the COM moves continuously, it is assumed that the x and z components are continuous $x_f = x_i$ and $z_f = z_i$. Furthermore, the change in the position of the foot is given as a control input $x_{si} = x_{sf} + u$. With the continuity equations for COM position and a control input for x_s , the new angle ϕ_i can be calculated as

$$\phi_i = \operatorname{atan}\left(\frac{l_f \sin \phi_f - u}{l_f \cos \phi_f}\right) \tag{16}$$

Where l_f is the length of the pendulum during the previous step. Note that the constant length l remains unchanged only during continuous phase. When the foot slips, for given position of COM, the leg has to extend accordingly to reach the control input u and its length is thus calculated as

$$l_i = l_f \frac{\cos \phi_f}{\cos \phi_i} \tag{17}$$

To determine \dot{x}_{si} and $\dot{\phi}_i$, two more equations are sought. The first equation comes from conservation of linear momentum in horizontal direction and the continuity in x, thus $\dot{x}_f = \dot{x}_i$. To obtain a second equation, an additional equation is prescribed depending on the slip condition. In case of non-slip conditions, the contact point velocity is assumed to be zero and in the case of slip, the rotational velocity is assumed zero. The missing two equations are thus written as

$$\dot{\phi}_i = \dot{\phi}_f \frac{l_f \cos \phi_f}{l_f \cos \phi_f}, \qquad \dot{x}_{si} = 0 \tag{18}$$

for non-slip conditions, and

$$\dot{\phi}_i = 0, \qquad \dot{x}_{si} = \dot{x}_{sf} + l_f \dot{\phi}_f \cos \phi_f \tag{19}$$

for slip conditions.

Another plausible treatment is to assume the conservation of total kinetic energy and then $\dot{z}_f = \dot{z}_i$. However, given the rigidity of the leg, this approach tends to result in non-realistic conditions close to singularity. If the foot is positioned in such a way that velocities \dot{z} and \dot{x} align with the leg, then the resulting angular velocity experiences singularity, that is, $\dot{\phi}_i \rightarrow \infty$.

Capturability concept

A framework for capturability was first presented by Koolen et al. [24]. For the reader's convenience, the basic idea is repeated here. A hybrid dynamic system is described by continuous dynamics $\dot{\mathbf{x}} = \mathbf{f}(\mathbf{x}, \mathbf{u})$, where \mathbf{x} is the state of the system and u is a possible control input, and discrete dynamics $\mathbf{x} \leftarrow \mathbf{g_i}(\mathbf{x})$ presents a discrete jump in x. A set X_{failed} , represents all of the failed states and should be avoided at all costs. A state x_0 is considered N-step capturable, if there exists at least one evolution starting at x_0 and containing N steps, the state variables set never reaches X_{failed} . Next, an N-step viable capture basin is defined as the set of all N-step capturable states. This is equivalently expressed as a set of all the initial states x_0 for which there is at least one evolution which leads to an (N-1)-step viable capture basin. The 0-step viable capture basin is the set of captured states. The system in such a basin is considered captured, in other words, such a system is in an equilibrium position and comes to a stop. Given a system with known x_0 and X_{failed} , we can define its capture points. A point on the ground is a N-step capture point, if and only if there exists at least one evolution starting at x_0 and containing a single step which leads to an (N-1)-step capturable state. The N-step capture region is then a set of all N-step capture points. It is important to note that choosing an N-step capture point for the next step is a necessary but not sufficient condition for reaching a captured state.

In this work we are use the concept of capturability with N=2. This means that after the system is set in motion with a set of initial conditions $\mathbf{x_0}$, we observe 2-step capture regions. In order to bring the system to a stop within two steps, the walker must take the first step in one of such regions. If there exists a 1-step capture region, we treat those as a special case of 2-step capture regions, where the second step is of zero size.

Initial conditions and foot placement

The parameters of the model are as follows: m=70 kg, l=1.2 m, and $J=10 \text{ kg m}^2$. The coefficient of friction and time between steps are $\mu=0.15$ and $t_1=0.45$ s. The largest distance of the step is chosen $u_{max}=0.8 \text{ m}$ in either direction. For all the simulations, the system is set in motion by initial state $\mathbf{x_0}=(\phi_0,\dot{\phi}_0,x_{s0},\dot{x}_{s0})$, where $\phi_0=-20^\circ,\dot{\phi}_0=70^\circ\text{s}^{-1},x_{s0}=0 \text{ m}$ and $\dot{x}_{s0}=0.3 \text{ m s}^{-1}$.

Initial conditions were deliberately chosen to emulate the common behavior of slip which presents the possibility of falling. Given those initial conditions, at the end of the first continuous phase, the system slips forward with $\dot{x_s} > 0$ and the angular velocity is negative $\dot{\phi} < 0$. In order to mitigate the slip, a step backwards to reduce x and increase $\ddot{\phi}$ and F_x has to be initiated. To obtain the capture regions, all the capture points have to be evaluated numerically by examining the behavior of the system for each positioning of the foot from 0 to 0.8 m behind the current standing foot with an increment of 5 mm. The locations of

the first step are noted and the system is propagated continuously through its standing phase. Depending on the foot placement, the biped walker might experience no slip, or slip in either direction. For that reason, the location of the foot placement for subsequent steps is not restricted to either positive or negative values but instead encompasses all the locations $|u| < u_{max}$. Thus we use $u \in (-0.8, 0.8)$ m with a 2 mm increment.

A captured state is determined as $\dot{x}_s=0,\ \phi=0$ and $\dot{\phi}=0$. Since the final position is only calculated for a set of discrete values for steps, the captured state condition is relaxed to $\dot{x}_s=0,\ |\phi|\leq\delta$ and $|\dot{\phi}|\leq\delta$ where δ is a small number. If at any time during the simulation, the value of the angle exceeds the limit $|\phi|>70^\circ$, the system is considered to have fallen and has entered $\mathbf{X}_{\mathrm{failed}}$.

RESULTS

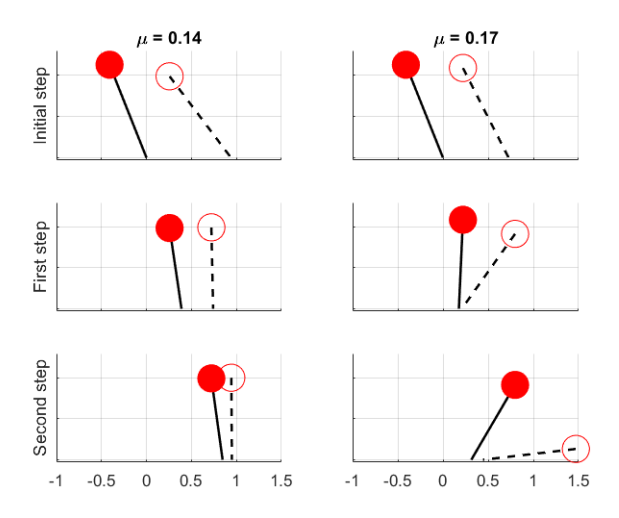


FIGURE 2. Snapshot of models with the same control input but different μ in motion. Solid and dashed lines show the beginning and the end of continuous phase respectively.

We present simulation results in this section. Fig. 2 shows snapshots of the model in motion. The solid line represents the position at the beginning of the continuous phase, right after the step was taken, while the dashed line represents the end of continuous phase immediately before the next step is taken. Thus the dashed model represents the system at an interval of t_1 after the solid model on the same plot. The topmost snapshots represent the first continuous phase that is set in motion by initial conditions. The middle snapshots show the system after the first step is taken while the bottom snapshots represent the propagation after the second step. The left and the right column have an

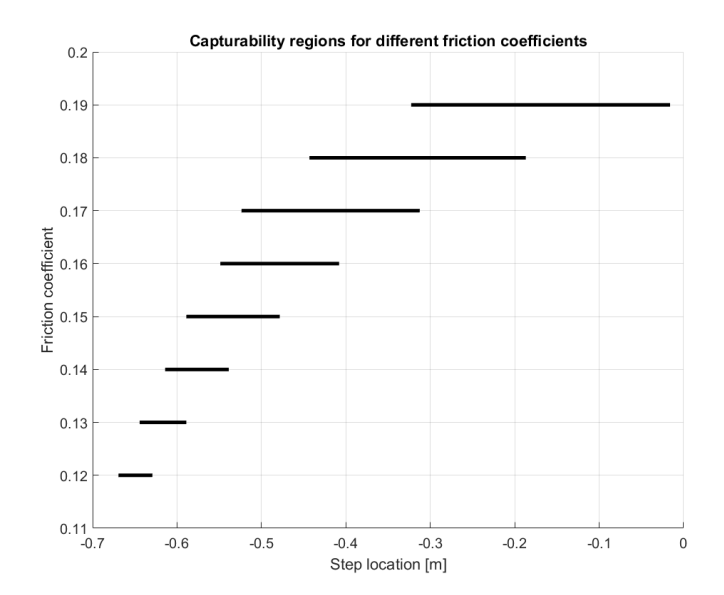


FIGURE 3. Capture regions in relation to μ . Each line represents the area of the ground where a walker with a given μ has to step in order to reach the captured state

identical control input, initial conditions and all the parameters. The coefficient of friction is $\mu=0.14$ for the left column and $\mu=0.17$ for the right column.

Fig. 2 represents the gait where the length of the steps are $u_1 = -0.55$ m and $u_2 = 0.104$ m. These values were chosen because they stabilize the walker with $\mu = 0.14$. Initially, the contact foot is placed at the point $x_s = 0$, however due to slip, the contact point moves forward and the COM moves downward. To counteract this movement, step u_1 is taken backwards and the system continues as shown in the second row of Fig. 2. Under the low friction condition, the system keeps slipping, while the higher friction ensures that the slip stops almost immediately. The next goal is to determine whether the point u_1 is a capture point for each of the cases. We demonstrate that by taking a forwards step u_2 , the low friction condition ($\mu = 0.14$) comes to rest, thus making the point u_1 a 2-step capture point. However, the same second step does not bring the high friction ($\mu = 0.17$) to equilibrium. In fact, no possible second step, would bring the high friction system to rest and thus, the point u_1 is not a 2-step capture point in case of $\mu = 0.17$.

Influence of coefficient of friction

In order to study capture regions, repeated calculation is performed for all possible step sizes. Similar calculation is repeated for different values of the friction coefficient and the results are presented in Fig. 3.

Fig. 3 shows the capture regions, where the abscissa is the location of the point on the ground and the ordinate is the value of

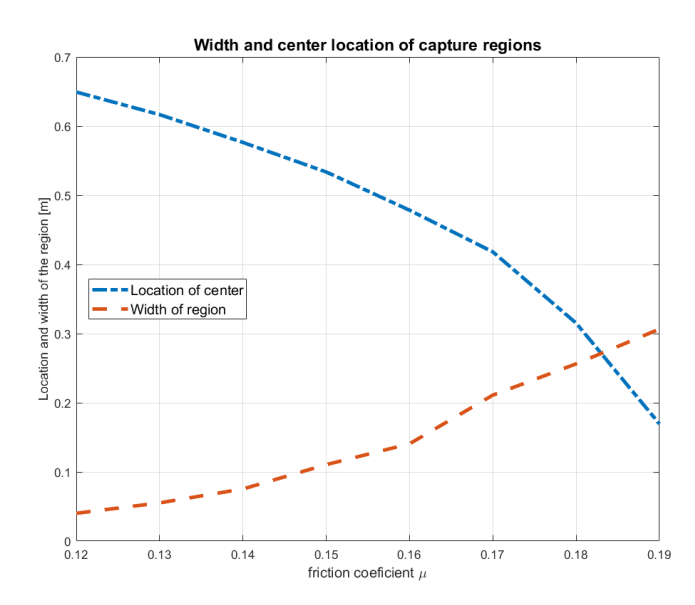


FIGURE 4. Size and location of capture regions with regards to coefficient of friction

 μ . It can be seen that the capture region moves further back when the values of the coefficient of friction decreases. Conversely, if the value of μ increases, the region moves forward, and the case of $\mu=0.2$ encompasses x=0, when the back step is no longer required for recovery. With further increasing the μ , the slip gets eliminated during the first step and no corrective action is needed when placing the foot.

Fig. 4 shows the same results in different representation. Instead of representing as straight lines, the capture regions are shown with two parameters: their width and the distance of the centers from the current foot position, which is defined as zero. This plot also shows that with decreasing μ , not only do the centers of regions move further back, but the capture regions also become narrower.

With lower μ , the rotation $|\dot{\phi}|$ is higher, thus requiring a longer step back to sufficiently lower the $|\dot{\phi}|$. On the other hand, if the step backwards is too large, a foot slip with $\dot{x}_s < 0$ occurs. Due to those constrains, capture regions get narrower with decreasing μ .

Influence of reaction time

The effects of varying step time on capture regions are similar but opposite to the effects of varying coefficient of friction.

Fig. 5 confirms that when reducing the time between steps, the required step back becomes shorter. Further, taking a step in a shorter amount of time allows for more variance in the positioning of the foot and still results in an equilibrium position. Fig. 6 illustrates the capture region locations and sizes as a function of step time duration. The relationship between μ and step time

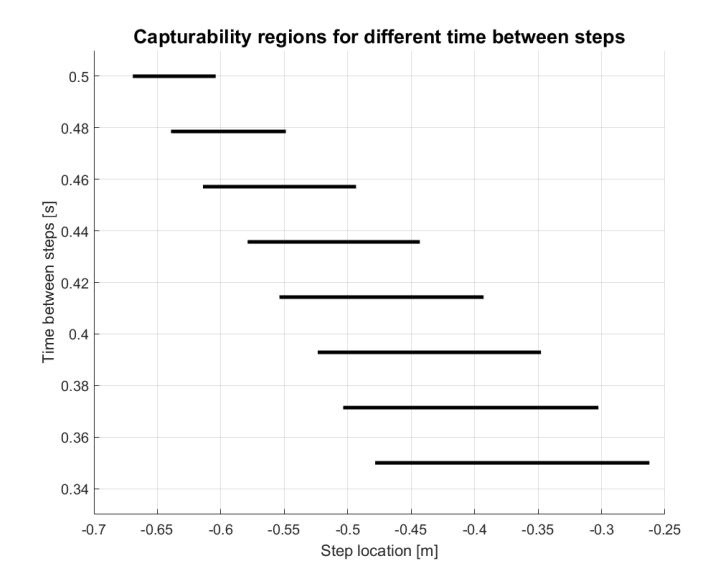


FIGURE 5. Capture regions in relation to time between two steps

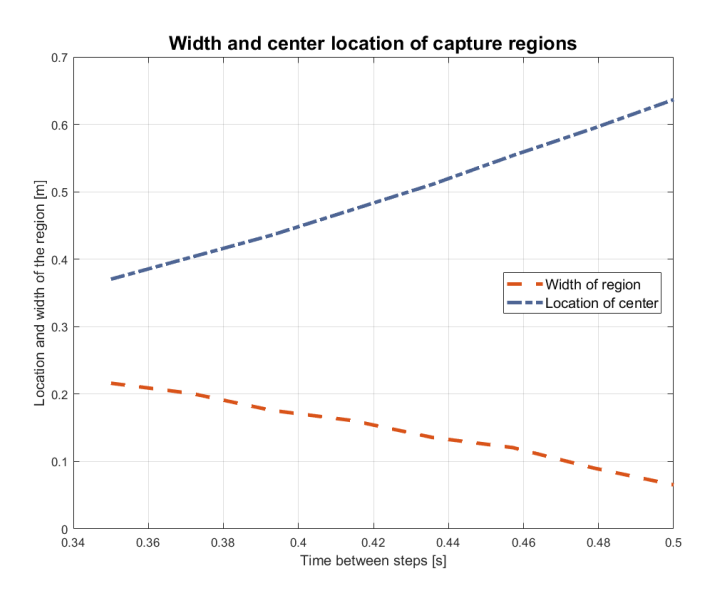


FIGURE 6. Size and location of capture regions with regards to time between steps

duration is apparent when comparing Figs. 4 and 6. Increasing the step time duration has similar effects as decreasing the coefficient of friction as they both narrow the capture regions and shift the regions backwards. The capture regions are identical on both plots centered at -0.54 m from standing foot when identical parameters $\mu=0.15$ and $t_1=0.45$ are considered. The width of the capture region is easily influenced by the friction coefficient, whilst the location of the regions changes more with time duration variation.

CONCLUSIONS

This paper presented a new inverted pendulum model that allows for the horizontal as well as the vertical movement of center of the mass. Such a model enabled a realistic gait study under slip conditions. Given a set of initial conditions, slip recovery was computed with varying parameters for the duration of a single step and the friction coefficient between the foot and the floor. It was found that lowering the coefficient of friction or increasing the time between steps has a similar two-fold effect. First, the required step has to be taken further away from previous standing foot in a direction opposite to the slip. Second, the leg has to be positioned more precisely. This implied that for a person to recover from slip, low friction and a large reaction time might present significant challenges. Those observations coincided with previous empirical knowledge from clinical studies.

ACKNOWLEDGMENTS

The work was supported in part by US NSF under awards CMMI-1334389 and CMMI-1762556

REFERENCES

- [1] Corso, P., Finkelstein, E., Miller, T., Fiebelkorn, I., and Zaloshnja, E., 2006. "Incidence and lifetime costs of injuries in the United States". *Injury Prevention*, 12(4), pp. 212–218.
- [2] Heinrich, S., Rapp, K., Rissmann, U., Becker, C., and König, H.-H., 2010. "Cost of falls in old age: a systematic review". *Osteoporosis Intl.*, *21*(6), pp. 891–902.
- [3] Redfern, M. S., Cham, R., Gielo-Perczak, K., Grönqvist, R., Hirvonen, M., Lanshammar, H., Pai, C. Y.-C., and Power, C., 2001. "Biomechanics of slips". *Ergonomics*, *44*(13), pp. 1138–1166.
- [4] Yang, F., and Pai, Y.-C., 2010. "Reactive control and its operation limits in responding to a novel slip in gait". *Ann. Biomed. Eng.*, **38**(10), pp. 3246–3256.
- [5] Trkov, M., Chen, K., Yi, J., and Liu, T., 2015. "Slip detection and prediction in human walking only using wearable inertial measurement units (IMUs)". In Proc. IEEE/ASME Int. Conf. Adv. Intelli. Mechatronics, pp. 854–859.
- [6] Trkov, M., Yi, J., Liu, T., and Li, K., 2018. "Shoe-floor interactions human walking with slips: Modeling and experiments". ASME J. Biomech. Eng., 140(3), pp. 031005– 1–031005–11.
- [7] Westervelt, E. R., Grizzle, J. W., Chevallereau, C., Choi, J. H., and Morris, B., 2007. Feedback Control of Dynamic Bipedal Robot Locomotion. CRC Press, Boca Raton, FL.
- [8] Martin, A. E., and Schmiedeler, J. P., 2014. "Predicting human walking gaits with a simple planar model". *J. Biomech.*, 47, pp. 1416–1421.

- [9] Chen, K., Trkov, M., and Yi, J., 2017. "Hybrid zero dynamics of human walking with foot slip". In Proc. Amer. Control Conf., pp. 2124–2129.
- [10] Golliday, C., and Hemami, H., 1977. "An approach to analyzing biped locomotion dynamics and designing robot locomotion controls". *IEEE Trans. Automat. Contr.*, 22(6), pp. 963–972.
- [11] Kajita, S., and Tani, K., 1991. "Study of dynamic biped locomotion on rugged terrain-derivation and application of the linear inverted pendulum mode". In Proc. IEEE Int. Conf. Robot. Autom., pp. 1405–1411.
- [12] Gomes, M., and Ruina, A., 2011. "Walking model with no energy cost". *Physical Review E, 83*(3), p. 032901.
- [13] Faraji, S., and Ijspeert, A. J., 2017. "3LP: a linear 3D-walking model including torso and swing dynamics". *Int. J. Robot. Res.*, 36(4), pp. 436–455.
- [14] Kajita, S., Kanehiro, F., Kaneko, K., Yokoi, K., and Hirukawa, H., 2001. "The 3d linear inverted pendulum mode: A simple modeling for a biped walking pattern generation". In Proc. IEEE/RSJ Int. Conf. Intell. Robot. Syst., pp. 239–246.
- [15] Koolen, T., Posa, M., and Tedrake, R., 2016. "Balance control using center of mass height variation: limitations imposed by unilateral contact". In Proc. IEEE Int. Conf. Humanoid Robots, pp. 8–15.
- [16] Dai, H., and Tedrake, R., 2016. "Planning robust walking motion on uneven terrain via convex optimization". In Proc. IEEE Int. Conf. Humanoid Robots, pp. 579–586.
- [17] Hirukawa, H., Hattori, S., Harada, K., Kajita, S., Kaneko, K., Kanehiro, F., Fujiwara, K., and Morisawa, M., 2006. "A universal stability criterion of the foot contact of legged robots-adios zmp". In Proc. IEEE Int. Conf. Robot. Autom., pp. 1976–1983.
- [18] Chen, K., Trkov, M., Yi, J., Zhang, Y., Liu, T., and Song, D., 2015. "A robotic bipedal model for human walking with slips". In Proc. IEEE Int. Conf. Robot. Autom., pp. 6301– 6306.
- [19] Chen, K., Trkov, M., Chen, S., Yi, J., and Liu, T., 2016. "Balance recovery control of human walking with foot slip". In Proc. Amer. Control Conf., pp. 4385–4390.
- [20] Hof, A. L., 2005. "The condition for dynamic stability". *J. Biomech.*, 38, pp. 1–8.
- [21] Pratt, J., Carff, J., Drakunov, S., and Goswami, A., 2006. "Capture point: A step toward humanoid push recovery". In Proc. IEEE Int. Conf. Humanoid Robots, pp. 200–207.
- [22] Englsberger, J., Ott, C., and Albu-Schäeffer, A., 2015. "Three-dimensional bipedal walking control based on divergent component of motion". *IEEE Trans. Robotics*, 31(2), pp. 355–368.
- [23] Khadiv, M., Herzog, A., Moosavian, S. A. A., and Righetti, L., 2017. "A robust walking controller based on online step location and duration optimization for bipedal

- locomotion". *Int. J. Robot. Res.* [Online]. Available: https://arxiv.org/abs/1704.01271.
- [24] Koolen, T., de Boer, T., Rebula, J., Goswami, A., and Pratt, J., 2012. "Capturability-based analysis and control of legged locomotion, Part 1: Theory and application to three simple gait models". *Int. J. Robot. Res.*, *31*(9), pp. 1094–1113.